

Exceptional point induced lasing dynamics in a non-Hermitian system

K. L. Zhang,¹ P. Wang,¹ and Z. Song^{1,*}

¹*School of Physics, Nankai University, Tianjin 300071, China*

Non-Hermitian systems exhibit many peculiar dynamic behaviors which never showed up in Hermitian systems. The existence of spectral singularity (SS) for a non-Hermitian scattering center provides a lasing mechanism in the context of quantum mechanics. In this paper we show exactly that a finite system at exceptional point (EP) can also provide an alternative laser solution. We investigate the dynamics of non-Hermitian Su-Schrieffer-Heeger (SSH) model around EP, based on the analysis of parity-time (\mathcal{PT}) and chiral-time (\mathcal{CT}) symmetries of the Hamiltonian. In contrast to the SS lasing mechanism for an infinite system, such an SSH chain acts as an active laser medium at threshold, within which a stationary particle emission can be fired anywhere, rather than a specific location at the non-Hermitian scattering center only. In addition, some relevant peculiar phenomena arising from interference between wave packets are revealed based on the analytical solutions.

I. INTRODUCTION

The recent development of non-Hermitian quantum mechanics [1–11] has opened up the perspective in several branches of physics [12–21]. The remarkable features of a non-Hermitian system is the violation of conservation law of the Dirac probability and the exceptional point (EP) or spectral singularity (SS). Based on the former, the complex potential is employed to describe open systems phenomenologically [22]. Furthermore, unconventional propagation of light associated with the gain/loss has been demonstrated by engineering effective non-Hermitian Hamiltonians in optical systems [23–25]. On the other hand, many unique optical phenomena have been observed around exceptional point (EP), ranging from loss-induced transparency [23], power oscillations violating left-right symmetry, low-power optical diodes [26], to single-mode laser [27, 28]. A fascinating phenomenon of non-Hermitian optical systems in the application aspect is the gain-induced detection, such as enhanced spontaneous emission [29], enhanced nanoparticle sensing [30] as well as the amplified transmission in the optomechanical system [31, 32]. Both theoretical and experimental works not only give an insight into the dynamical property of the non-Hermitian Hamiltonian but also provide a platform to implement the optical phenomenon.

In this paper, using the exact solutions, we introduce a mechanism for self-sustained emission in finite non-Hermitian systems at the EP. We show that, without the existence of SS in a scattering system, one is able to obtain a class of lasing solutions. For such solutions, a lasing mode is fired at any location of the system, which acts as an active lasing medium, rather than the non-Hermitian scattering center only in the context of SS regime. In order to demonstrate the EP lasing dynamics, we consider a one-dimensional (1D) \mathcal{PT} -symmetry non-Hermitian Su-Schrieffer-Heeger (SSH) model [33]. The exact solution is obtained in the strong dimer-

ization limit, which shows that the equal-level-spacing high-frequency standing-wave modes (EHSM) [34] can be achieved in a chain system when the corresponding ring system is tuned at the exceptional point (EP), as depicted schematically in Fig. 1. Such a deliberately designed system supports some peculiar dynamics for a localized initial state, which originates from the combination of the time evolutions involving nonzero energy levels and Jordan block of the corresponding SSH ring lattice within a finite time scale. Based on the analysis of parity-time (\mathcal{PT}) and chiral-time (\mathcal{CT}) symmetries of the Hamiltonian, a class of solutions are constructed based on energy levels around the zero energy. Such a class of states involve wave packets with different shapes and locations, which support the stationary lasing dynamics. In addition, it is found that the superposition of these states exhibit some counterintuitive dynamical behaviors. Although the system is non-interacting, a delicate design of the interference process results in the phenomena of wave packet-pair annihilation and creation.

The remainder of this paper is organized as follows. In Sec. II, we present a non-Hermitian SSH chain model and the formulation of approximate diagonalization. In Sec. III, we investigate the generic dynamics for a system with parity-time (\mathcal{PT}) and chiral-time (\mathcal{CT}) symmetries Hamiltonian. Section IV presents the laser solution and reveals the lasing dynamics for specific initial localized states. Section V demonstrates some peculiar dynamical behaviors in the present system. Finally, we give a summary and discussion in Sec. VI.

II. MODEL AND SOLUTION

As beginning, we briefly summarize known properties of the 1D non-Hermitian SSH model with staggered balanced gain and loss. It has been studied systematically in the previous work [33, 34]. The simplest tight-binding

* songtc@nankai.edu.cn

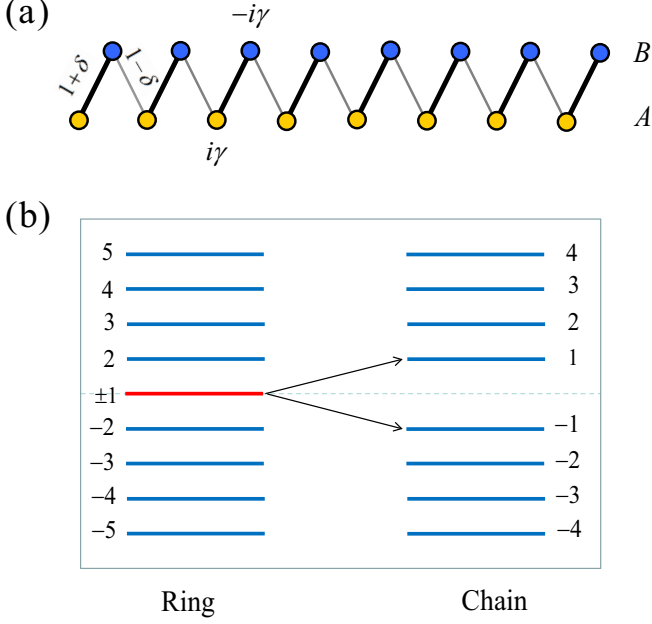


FIG. 1. (Color online) (a) Schematic for 1D non-Hermitian SSH model. It consists of two sublattice, A (golden) and B (blue). Black thick and gray thin lines indicate the hopping between two nearest neighbor sites with amplitudes $(1 + \delta)$ and $(1 - \delta)$, respectively. Two sublattices have opposite site imaginary potentials $\pm i\gamma$, representing the physical gain and loss. It has \mathcal{PT} -symmetry and can have full real spectrum in the case of $1 > \delta > 0$ and $\gamma < \gamma_c$ (see text). (b) The spectra of the non-Hermitian SSH model at $\gamma = \gamma_c$ with periodic and open boundary (by breaking one of the weak hopping term) conditions, respectively. In both two cases, energy levels near zero are equal-spacing. For ring system two zero level coalescence which is splitted into two levels when the open boundary condition is imposed.

model with these features is

$$H = (1 + \delta) \sum_{j=1}^N a_j^\dagger b_j + (1 - \delta) \sum_{j=1}^{N-1 \text{ or } N} b_j^\dagger a_{j+1} + \text{H.c.} + i\gamma \sum_{j=1}^N (a_j^\dagger a_j - b_j^\dagger b_j), \quad (1)$$

where δ and $i\gamma$, are the distortion factor with unit tunneling constant and the alternating imaginary potential magnitude, respectively. Here a_l^\dagger and b_l^\dagger are the creation operator of the particle at the l th site in A and B sublattices. The particle can be fermion or boson, depending on their own commutation relations. In the second term, two kinds of summation can be taken, correspond to open and periodic boundary conditions. For nonzero γ , it is still a \mathcal{PT} -symmetry. Here, the time reversal operation \mathcal{T} is such that $\mathcal{T}i\mathcal{T} = -i$, while the effect of the parity is such that $\mathcal{P}a_l\mathcal{P} = b_{N+1-l}$ and $\mathcal{P}b_l\mathcal{P} = a_{N+1-l}$. Applying operators \mathcal{P} and \mathcal{T} on the Hamiltonian (1), one has

$[\mathcal{T}, H] \neq 0$ and $[\mathcal{P}, H] \neq 0$, but

$$[\mathcal{PT}, H] = 0. \quad (2)$$

In parallel, H also has chiral-time symmetry

$$\{\mathcal{CT}, H\} = 0, \quad (3)$$

where operator \mathcal{C} is defined as

$$\mathcal{C}a_j\mathcal{C}^{-1} = a_j, \mathcal{C}b_j\mathcal{C}^{-1} = -b_j. \quad (4)$$

The situation here is a little different from the case associated with \mathcal{PT} symmetry. In quantum mechanics, we say that a Hamiltonian H has a symmetry represented by a operator \mathcal{L} if $[H, \mathcal{L}] = 0$. The word ‘‘symmetry’’ is also used in a different sense in condensed matter physics. We say that a system with Hamiltonian H has chiral symmetry, if $\{H, \mathcal{C}\} = 0$. The physics of \mathcal{C} depends on the model discussed [35–40]. A non-Hermitian system with \mathcal{CT} symmetry has been systematically studied in Ref. [41].

According to the non-Hermitian quantum theory, such a Hamiltonian may have fully real spectrum within a certain parameter region. The boundary of the region is the critical point of quantum phase transition associated with \mathcal{PT} -symmetry breaking. For the system with periodic boundary condition, the critical point occurs at $\gamma = \gamma_c = 2\delta$, which is also referred as to EP [33]. According to the Appendix in Ref. [34], in the strong dimerization limit $1 + \delta \gg 1 - \delta$, the Hamiltonian with open boundary condition can be diagonalized approximately and the single-particle eigen vectors for $\gamma = \gamma_c$ can be expressed as

$$|\psi_n^\pm\rangle = \sqrt{\frac{\pm(-1)^N}{N+1}} \sum_{j=1}^N (-1)^j \sin(kj) \times \left(e^{\pm i\varphi_k/2} a_j^\dagger \pm e^{\mp i\varphi_k/2} b_j^\dagger \right) |0\rangle, \quad (5)$$

where k is defined as

$$k = \frac{n\pi}{N+1}, \quad n \in [1, N]. \quad (6)$$

The corresponding eigen energy is

$$\varepsilon_k = \sqrt{[(1 + \delta) - (1 - \delta) \cos k]^2 - \gamma_c^2}, \quad (7)$$

and

$$\tan \varphi_k = \frac{\gamma_c}{\varepsilon_k}. \quad (8)$$

We note that γ_c is no longer the EP for the open chain and we find that the energy levels can be expressed as

$$E_n^\pm = \pm n\omega, \quad \omega = \frac{\sqrt{2\delta(1-\delta)}\pi}{N+1}, \quad (9)$$

approximately for not large n . Here $|\psi_n^\pm\rangle$ is normalized in the framework of Dirac inner product, i.e., $\langle \psi_m^\pm | \psi_n^\pm \rangle =$

δ_{mn} . It indicates that the spectrum ε_k consists of two branches separated by an energy gap $\Delta = 2\omega$, which ensures the existence of the equal-level-spacing standing-wave modes (ESM) around zero energy. In this model, the value of γ_c is necessary for achieving a set of eigenstates as ESM, which is crucial for the construction of our target state. In addition, the deliberate expression of the set of eigenvector $\{|\psi_n^\pm\rangle\}$ makes it satisfies

$$\mathcal{PT}|\psi_n^\pm\rangle = (-1)^n |\psi_n^\pm\rangle, \quad (10)$$

and

$$\mathcal{CT}|\psi_n^\pm\rangle = -i|\psi_n^\mp\rangle, \quad (11)$$

which will be used to analyze the dynamics of the system in the following sections. It is familiar to the operator \mathcal{P} or \mathcal{C} in a system with reflection symmetry, which is widely used in physics. However, we would like to point out that here \mathcal{T} is an antilinear operator, which has not a definite eigenvalue for a given eigenstate. In the previous work [34], we have studied a similar model and the corresponding dynamics. The spectrum consists of two branches separated by an energy gap $\Delta \gtrsim 0$ and then it may or not contain the coalescing level with zero energy. In addition, since only one branch of levels are involved in the initial states, the obtained result is not sensitive to the precise value of the gap Δ . However, in the present work we will show that the existence of stationary laser mode strongly depends on the value of Δ , or γ .

III. QUASI-SYMMETRIC DYNAMICS

Before the investigation for the dynamics of some specific initial state, we would like to study some general properties of dynamics for a \mathcal{PT} and \mathcal{CT} symmetric system, which is helpful for the subsequent discussions. In the following two sections, we will reveal two features of dynamics, which are related to the symmetries of the system, but not exact results. The first one is a quasi symmetric time evolution and the second one is about time-reflection symmetry. The obtained result in this section is applicable for more general system.

Unlike the symmetry related to a linear operator \mathcal{L} , here \mathcal{PT} and \mathcal{CT} are anti-linear operators, which act in a different way in the time evolution for a symmetric initial state. Consider a Hamiltonian \mathcal{H} has \mathcal{L} , \mathcal{PT} and \mathcal{CT} symmetries, i.e.,

$$[\mathcal{L}, \mathcal{H}] = [\mathcal{PT}, \mathcal{H}] = \{\mathcal{CT}, \mathcal{H}\} = 0, \quad (12)$$

respectively. An initial state $|\psi(0)\rangle$ is taken as the eigenstate of \mathcal{L} , \mathcal{PT} and \mathcal{CT} , e.g.,

$$\mathcal{L}|\psi(0)\rangle = \mathcal{PT}|\psi(0)\rangle = \mathcal{CT}|\psi(0)\rangle = |\psi(0)\rangle. \quad (13)$$

We are interested in the symmetry of the evolved state $|\psi(t)\rangle = e^{-i\mathcal{H}t}|\psi(0)\rangle$. Direct derivations show that

$$\mathcal{L}|\psi(t)\rangle = \mathcal{CT}|\psi(t)\rangle = |\psi(t)\rangle, \quad (14)$$

$$\mathcal{PT}|\psi(t)\rangle = |\psi(-t)\rangle, \quad (15)$$

which indicate that the evolved state may not maintain the initial symmetry associated with an anti-linear operator.

Applying the above analysis to the present SSH model, we will have following observations. Here \mathcal{L} can be taken as operator $\sum_{j=1}^N (a_j^\dagger a_j + b_j^\dagger b_j)$ as an example, which obeys the Eq. (14). For the \mathcal{PT} symmetric initial state, we have the symmetric Dirac probability distribution

$$\begin{aligned} |\langle j|\psi(0)\rangle|^2 &= |\langle j|\mathcal{PT}|\psi(0)\rangle|^2 \\ &= |\langle 2N+1-j|\psi(0)\rangle|^2. \end{aligned} \quad (16)$$

However, for the evolved state we have

$$\begin{aligned} |\langle j|\psi(t)\rangle|^2 &= \left| \langle j|(\mathcal{PT})^{-1} e^{i\mathcal{H}t} \mathcal{PT} |\psi(0)\rangle \right|^2 \\ &= |\langle 2N+1-j|\psi(-t)\rangle|^2, \end{aligned} \quad (17)$$

which cannot guarantee a symmetric probability profile.

Now we will show that the time evolution is symmetric approximately for a class of initial state. For small n , the approximate eigenstate of the Hamiltonian with even N reads

$$\begin{aligned} |\psi_n^\pm\rangle &\approx e^{\pm i\pi/4} \sqrt{\frac{\pm 1}{N+1}} \sum_{j=1}^N (-1)^j \sin(kj) \\ &\times (a_j^\dagger - ib_j^\dagger) |0\rangle, \end{aligned} \quad (18)$$

by taking

$$\varphi_k \approx \frac{\pi}{2}. \quad (19)$$

The implication of the approximation is clear that two eigenstate $|\psi_n^\pm\rangle$ with opposite energy $\pm E_n$ have the same expression. The time evolution of $|\psi_n^\pm\rangle$ is

$$\begin{aligned} e^{-i\mathcal{H}t} |\psi_n^\pm\rangle &\approx e^{\mp iE_n t} e^{\pm i\pi/4} \sqrt{\frac{\pm 1}{N+1}} \sum_{j=1}^N (-1)^j \\ &\times \sin(kj) (a_j^\dagger - ib_j^\dagger) |0\rangle. \end{aligned} \quad (20)$$

Furthermore, for a \mathcal{CT} symmetric state, e.g.

$$|\varphi_+\rangle = \sum_n c_n^+ (|\psi_n^+\rangle + |\psi_n^-\rangle), \quad (21)$$

with real c_n^+ , we have

$$\begin{aligned} e^{-i\mathcal{H}t} |\varphi_+\rangle &= \sum_{n=1} c_n^+ (e^{-iE_n t} |\psi_n^+\rangle + e^{iE_n t} |\psi_n^-\rangle) \\ &\approx \sqrt{\frac{1}{N+1}} \sum_{j=1}^N f(j, t) (a_j^\dagger - ib_j^\dagger) |0\rangle, \end{aligned} \quad (22)$$

where

$$f(j, t) = \sum_n (-1)^j c_n^+ (e^{-iE_n t} e^{i\pi/4} + i.c.c.) \sin(kj). \quad (23)$$

Function $\sin(kj)$ is odd (even) function about the center of the chain when n is even (odd). If the $|\varphi_+\rangle$ is a \mathcal{PT} symmetric state, the summation in $f(j, t)$ runs over even (or odd) n only. Function $f(j, t)$ is also symmetric due to the fact that any combination of odd (even) functions is also an odd (even) function. Then probability $|\langle 0|(a_j + ib_j)e^{-iHt}|\varphi_+\rangle|^2$ is a symmetric function, i.e.,

$$|\langle j|\psi(t)\rangle|^2 \approx |\langle 2N+1-j|\psi(t)\rangle|^2. \quad (24)$$

Together with Eq. (17), we have

$$|\langle j|\psi(t)\rangle|^2 \approx |\langle j|\psi(-t)\rangle|^2, \quad (25)$$

which indicates that the time evolution has time-reflection symmetry about zero t .

We conclude that, the evolved state has symmetric probability distribution and time-reflection symmetry if the initial state satisfies three conditions, (i) \mathcal{PT} symmetry, (ii) \mathcal{CT} symmetry, (iii) involving very small n . We would like to point out that these results are approximate rather than exact, which are referred as to quasi symmetric dynamics. This result is important to construct and characterize the laser mode in the present non-Hermitian SSH chain.

IV. LASING DYNAMICS

In this section, we will investigate the dynamics for a class of specific state. We focus on the initial state satisfying three conditions: (i) The Dirac probability distribution is localized in the coordinate space; (ii) The coefficient c_n^σ is non-vanishing only for small n ; (iii) It has \mathcal{CT} symmetry. It is expected that such kinds of initial state may possess lasing dynamics due to the following reasons: Although the non-Hermitian SSH chain does not have EP at γ_c , its corresponding ring system has an EP at zero energy. However, a local wave packet does not know whether boundary condition is open or periodic unless its final state touches the boundary. Then the wave

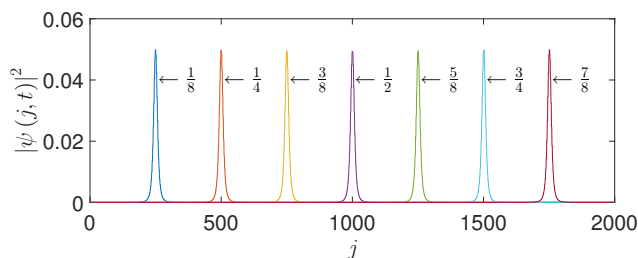


FIG. 2. (Color online) Profiles of initial states from the plot of Eq. (31) with $\kappa_0 = \pi/8, \pi/4, \dots, 7\pi/8$, respectively. It shows that the initial states are all localized with the identical shape in coordinate space and the central position is the linear function of κ_0 . The parameters are $2N = 2000$, $\delta = 0.9$, $\gamma = 1.8$ and $q = 0.02$.

packet should partially exhibit the EP dynamics which obeys the time evolution in a Jordan block [42–44], when the initial state $|\psi(0)\rangle$ has a component of the coalescing eigenstates of the SSH ring at EP. On the other hand, the above condition (ii) ensures that $|\psi(0)\rangle$ may probably contain such the coalescing component. From the analysis of the last section, conditions (ii) and (iii) constrain the evolved state to possess symmetric probability distribution and time-reflection symmetry, which make the dynamics more convenient to describe.

Before focusing on specific initial states, we study some features of time evolution for an initial state satisfying the above condition (ii). For small n , we have

$$|\psi(m\tau)\rangle = \sum_{n=1, \sigma=\pm} c_n^\sigma \exp(-i2nm\sigma\pi) |\psi_n^\sigma\rangle = |\psi(0)\rangle, \quad (26)$$

where

$$\tau = \frac{2\pi}{\omega} = \frac{2(N+1)}{\sqrt{2\delta(1-\delta)}}, \quad (27)$$

and m is an integer. It indicates that the initial state $|\psi(m\tau)\rangle$ revivals periodically with period τ . This property is not the direct result from the symmetry of the system. In addition, for the present model, we have

$$\begin{aligned} \left| \psi \left[\left(m + \frac{1}{2} \right) \tau \right] \right\rangle &= \sum_{n=1, \sigma=\pm} c_n^\sigma \exp(-in\sigma\pi) |\psi_n^\sigma\rangle \\ &= \sum_{n=1, \sigma=\pm} c_n^\sigma \mathcal{PT} |\psi_n^\sigma\rangle, \end{aligned} \quad (28)$$

based on Eq. (10). Specifically, for a class of initial states with a set of real (or total imaginary) $\{c_n^\sigma\}$, we have

$$\left| \psi \left[\left(m + \frac{1}{2} \right) \tau \right] \right\rangle = \mathcal{PT} |\psi(0)\rangle, \quad (29)$$

i.e., such states revival periodically at the symmetric position with period $\tau/2$ [45]. On the other hand, the dynamics of a Jordan block should exhibit increasing probability with a power law [42–44]. The combination of the two results gives us the following statement. In general, the probability should experience both an increasing and decreasing process within the time scale $\tau/2$. It accords with the prediction of dynamics with time-reflection symmetry.

Now we construct a class of initial states which meet the above three conditions. We will show that such states exhibit lasing dynamics during the time evolution. The initial state has the form

$$c_n^\sigma = \sigma \Lambda \sin(n\kappa_0) \frac{\exp(-qn)}{n}, \quad (30)$$

where Λ is a normalization constant, $q \geq 0$, and $\kappa_0 \in (0, \pi)$ are related to the shape and position of the initial state,

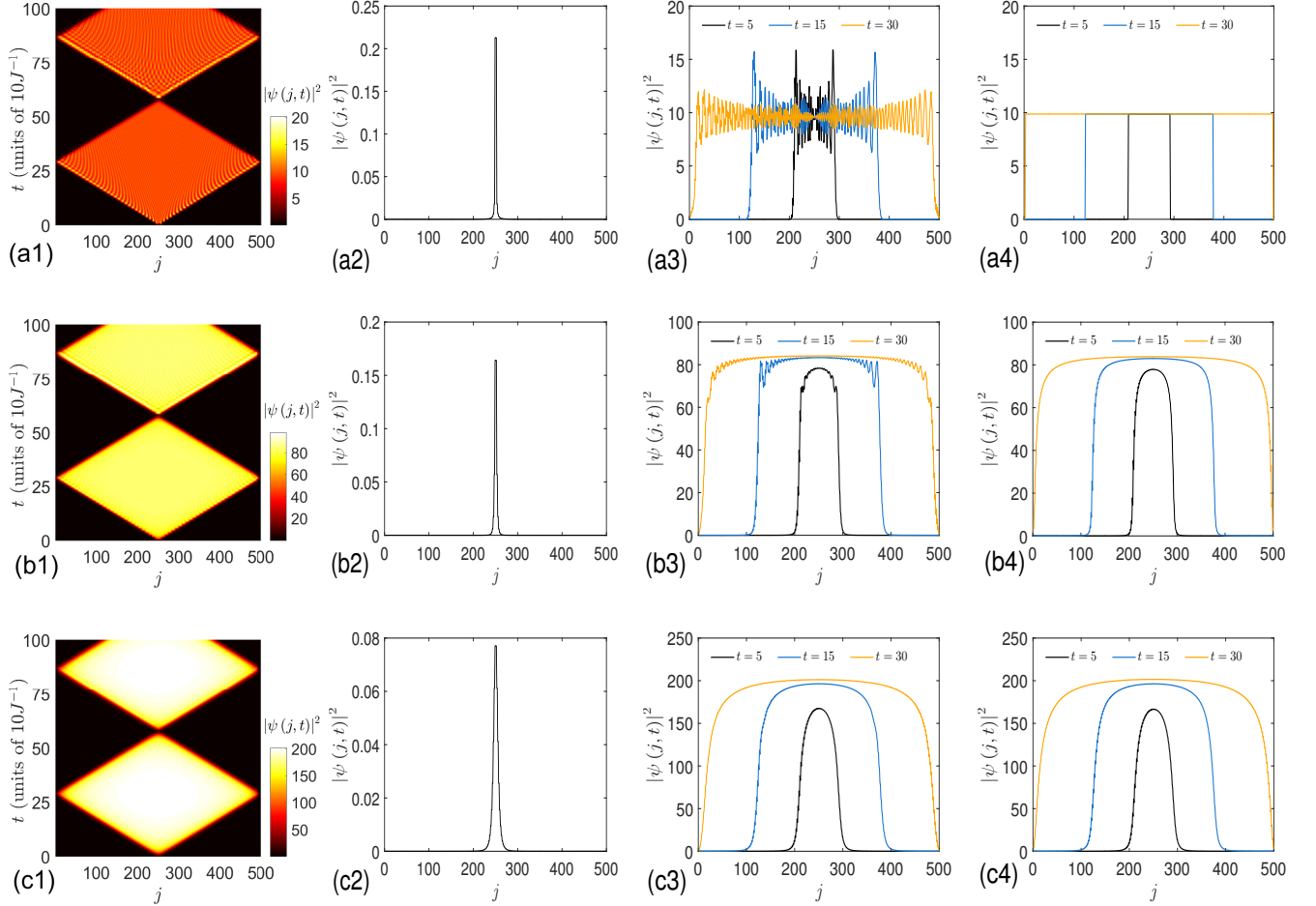


FIG. 3. (Color online) Profiles of evolved wave packets for initial states expressed in Eq. (31) with $\kappa_0 = \pi/2$ and several typical q values. $q = 0$ for (a1,a2,a3,a4), $q = 0.02$ for (b1,b2,b3,b4), and $q = 0.05$ for (c1,c2,c3,c4). (a1,b1,c1) Three-dimensional plots of evolved states for initial states plotted in (a2,b2,c2) obtained by numerical simulations. (a2,b2,c2) Plots of initial states from Eq. (31). (a3,b3,c3) Profiles of evolved states at several instants obtained by numerical simulations. (a4,b4,c4) The same as (a3,b3,c3) but obtained by analytical expression in Eq. (32). The parameters for the SSH chain are $2N = 500$, $\delta = 0.9$ and $\gamma = 1.8$. The time is in units of $10J^{-1}$, where J is the scale of the Hamiltonian and we take $J = 1$. The analytical expressions accord with the numerical results well, especially for non-zero q . It shows that the evolved states are flat-top (rectangular shape for zero q) with the uniformly increasing width, exhibiting stationary lasing dynamics before touching the boundary.

respectively. Obviously, c_n^σ is real and vanishing for large n . We note that the initial state

$$|\psi(0)\rangle = \Lambda \sum_{n=1, \sigma=\pm}^N \sigma \sin(n\kappa_0) \frac{\exp(-qn)}{n} |\psi_n^\sigma\rangle, \quad (31)$$

has both \mathcal{PT} and \mathcal{CT} symmetries for the case with $\kappa_0 = \pi/2$. To demonstrate the localization of $|\psi(0)\rangle$ in the coordinate space, we plot the profile of $|\psi(0)\rangle$ with several typical κ_0 in Fig. 2. It indicates that $|\psi(0)\rangle$ is a local wave packet with the center position $2N(\kappa_0/\pi)$. The time evolution of such local initial is independent of the initial position within a certain time scale. Then we can focus on the state $|\psi(0)\rangle$ with $\kappa_0 = \pi/2$. The evolved state always has symmetric profile in real space. Such kind of symmetric dynamics is convenient for analytical analysis and the obtained result can be applied

to the case with $\kappa_0 \neq \pi/2$ by a simple translation due to the locality of the evolved state.

To estimate the profile of the evolved state, we derive the evolved wave vector in the following compact form

$$|\psi(t)\rangle \approx \Lambda_N \sum_{j=1}^N \sum_{\rho, v, \eta=\pm 1} \arctan\left(\frac{\sin\theta}{e^q - \cos\theta}\right) \times (-1)^j \rho v \eta e^{i\eta\pi/4} \left| 2j - \frac{1}{2}(1-\eta) \right\rangle, \quad (32)$$

where $\Lambda_N = \frac{\Lambda}{2} \sqrt{(-1)^N / (N+1)}$ and

$$\theta = \rho\kappa_0 + \frac{v\pi j}{N+1} + \omega t - \frac{\eta}{4\delta}. \quad (33)$$

In Fig. 3, the profiles of $|\langle l|\psi(t)\rangle|^2$ are plotted, which are

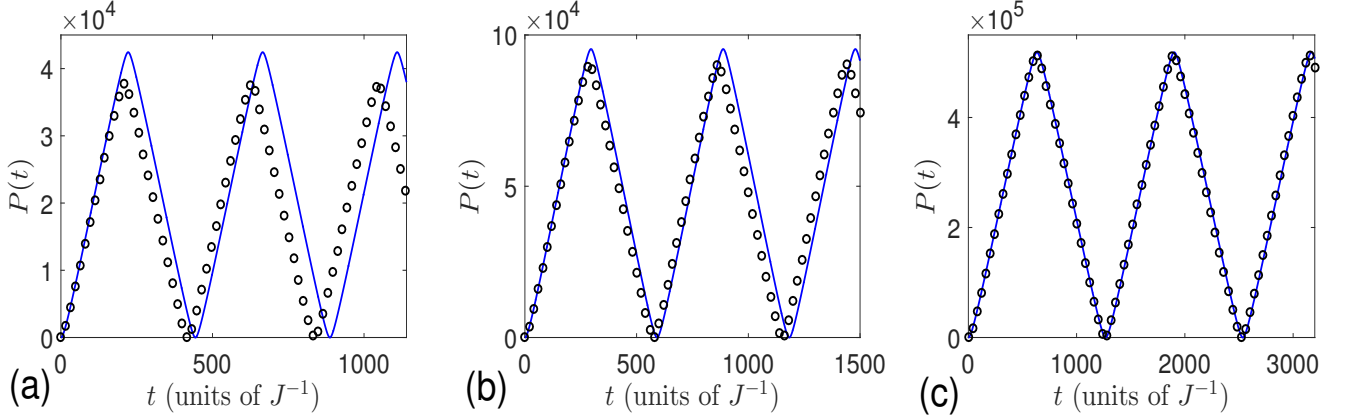


FIG. 4. (Color online) Plots of $P(t)$ obtained by numerical simulations (empty circle) and analytical expression (solid line) in Eq. (36). The parameters for the SSH chain are $2N = 500$, $\gamma = 2\delta$, and (a) $\delta = 0.8$, (b) $\delta = 0.9$, (c) $\delta = 0.98$, respectively. The initial states are taken the form in Eq. (31) with $\kappa_0 = \pi/2$ and $q = 0.05$. It shows that $P(t)$ is a triangle wave with period $\tau = 2(N + 1)/\sqrt{2\delta(1 - \delta)}$. The analytical expressions accord with the numerical results well, especially for the cases with strong dimerization.

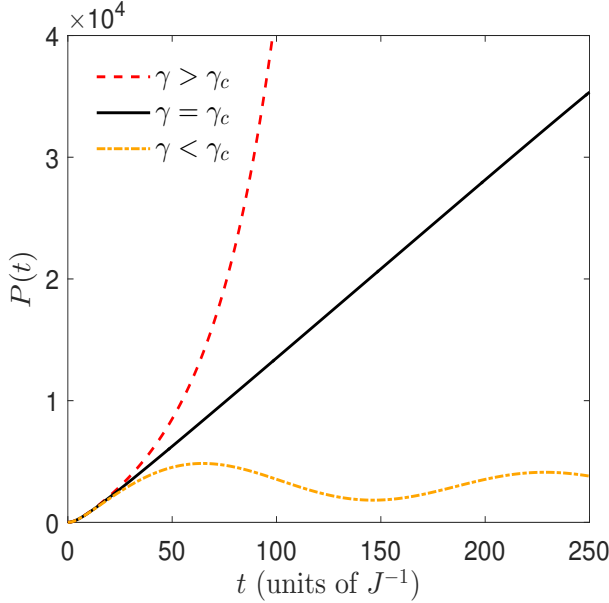


FIG. 5. (Color online) Plots of $P(t)$ obtained by numerical simulations for three typical values of γ . The parameters for the SSH chain are $2N = 500$, $\delta = 0.9$ and $\gamma_c = 1.8$. The initial states are taken the form in Eq. (31) with $\kappa_0 = \pi/2$, and $q = 0.02$. We can see that $P(t)$ is exponential for $\gamma > \gamma_c$, linear for $\gamma = \gamma_c$, and oscillation for $\gamma < \gamma_c$, respectively. It indicates that $\gamma = \gamma_c$ serves as the threshold of the active laser medium.

obtained by numerical simulations and approximate analytical expression in Eq. (32). It shows that the evolved state is a flat-top wave packet with uniformly increasing width. After bouncing from the two ends of the chain, it turns back to the initial state and starts the next cycling. This observation can be explained by the following

analysis for special case.

When $q = 0$, the expression of the evolved state reduces to

$$|\psi(t)\rangle \approx \frac{\Lambda_N}{2} \sum_{j=1}^N \sum_{\rho, \nu, \eta = \pm 1} (-1)^j \rho \nu \eta e^{i\eta\pi/4} r(\theta) \times \left| 2j - \frac{1}{2}(1 - \eta) \right\rangle, \quad (34)$$

where $r(x)$ is a periodic triangular function defined as:

$$r(x) = (\pi - x)/2 + n\pi, \quad x \in [0, 2\pi) + 2\pi n, \quad (35)$$

with $n \in \mathbb{Z}$. For $\kappa_0 = \pi/2$, the Dirac norm of the evolved state is

$$P(t) = \langle \psi(t) | \psi(t) \rangle \approx -\frac{\Lambda^2 e^{-2q}}{2} \text{Re} \left[e^{-i2\omega t} \Phi \left(e^{-4(q+i\omega t)}, 2, \frac{1}{2} \right) \right] + \Lambda^2 \sum_{\sigma = \pm} \sigma \text{Li}_2(\sigma e^{-2q}), \quad (36)$$

where $\Phi(z, s, \alpha) = \sum_{n=0}^{\infty} z^n / (n + \alpha)^s$ is the Lerch transcendental function and $\text{Li}_n(z) = \sum_{k=1}^{\infty} z^k / k^n$ is the Polylogarithm function. In particular, taking $q = 0$, the Dirac norm $P(t)$ becomes a triangular wave

$$P(t) \approx \frac{2\Lambda^2 \pi^2}{\tau} \begin{cases} t - n\tau/2, & t \in [0, \tau/4) + n\tau/2 \\ -t + (n+1)\tau/2, & t \in [\tau/4, \tau/2) + n\tau/2 \end{cases}, \quad (37)$$

with $n \in \mathbb{Z}$. As expected, it is the direct results of the uniform expanding flat-top wave packet. We also plot the function $P(t)$ from Eq. (36) and numerical simulation for several typical values of δ in Fig. 4, which indicates that our analytical result accords the numerical result well, especially for strong dimerization.

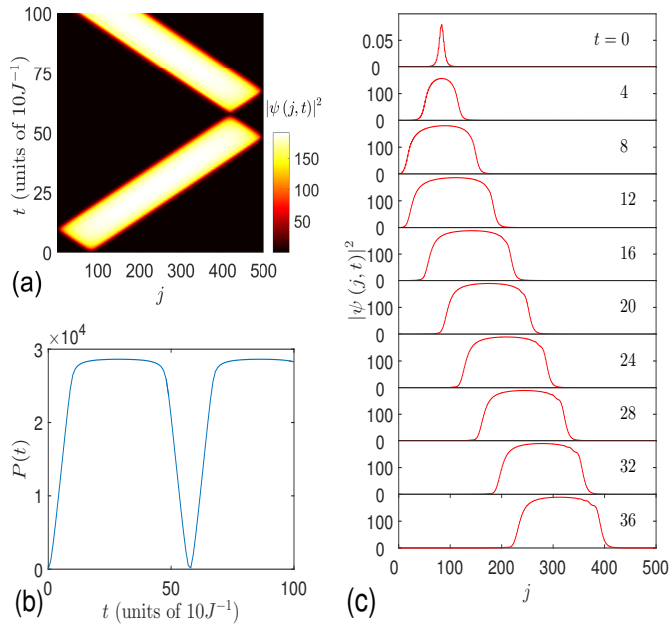


FIG. 6. (Color online) (a) Three-dimensional plots of evolved wave packets for initial states expressed in Eq. (31) with $\kappa_0 = \pi/6$ and $q = 0.05$, obtained by numerical simulation. (b) Plot of $P(t)$ for the time evolutions for (a). (c) The profiles of the evolved wave packet at several typical instants. The parameters for the SSH chain are $2N = 500$, $\delta = 0.9$ and $\gamma = 1.8$. It shows that the evolved states becomes a travelling wave packet after the first reflection on the one side, i.e., it propagates as a translational motion, preserving the probability before the subsequent reflection on the other side.

Obviously, such a stationary solution is related to the condition $\gamma = \gamma_c$. It is natural to ask what happens when γ deviates from γ_c . To answer this question, numerical simulations are performed by exact diagonalization. We plot the total probability as function of time for three cases in Fig. 5. It shows that the plot is exponential, linear, and oscillation for $\gamma > \gamma_c$, $\gamma = \gamma_c$, and $\gamma < \gamma_c$, respectively. It indicates that γ_c is the threshold for the lasing medium.

It is presumable that the lasing dynamics is independent of the position of the initial state if the chain is large enough. It differ from the lasing mechanics based on the SS in a non-Hermitian scattering center, in which only the scattering center acts as the active lasing medium. The underlying mechanism is the translational symmetry and the existence of EP in the bulk region of the chain.

V. PROBABILITY PRESERVING AND ELASTIC COLLISION

From the analysis in last section, we find that the extending rectangular wave or flat-top wave packet bounds back at two ends of the chain. We note that there are two features in the reflection process: (i) There is no interference pattern (standing wave) as usual. (ii) This process acts like a time-reflection one, i.e., the profiles of input and output are identical. In this section, we will study the underlying mechanism of this phenomenon. For this purpose, it will be convenient to think in terms of symmetric case and extends the conclusion to a general case, i.e., taking the case with $\kappa_0 = \pi/2$. In this case, the initial state is superposition of eigen states with small odd n . These eigen states are all long wave-length standing wave, the superposition of which have no ability to form interference pattern with small-frequency.

On the other hand, Fig. 3 and analytical analysis show that two edges of the flat-top wave packet touch the two ends of the chain at instant $t = \tau/4$. We note that

$$|\psi(\tau/4)\rangle = \sum_{n=1, \sigma=\pm} c_{2n-1}^{\sigma} \exp(-in\sigma\pi) i\sigma |\psi_{2n-1}^{\sigma}\rangle, \quad (38)$$

which are both \mathcal{PT} and \mathcal{CT} symmetric, satisfying

$$\mathcal{PT} |\psi(\tau/4)\rangle = |\psi(\tau/4)\rangle, \quad (39)$$

$$\mathcal{CT} |\psi(\tau/4)\rangle = i |\psi(\tau/4)\rangle, \quad (40)$$

taking $|\psi(\tau/4)\rangle$ as initial state, and using the conclusion (Eq. (25)) of Sec. III, we obtain

$$|\langle j |\psi(\tau/4 + \Delta t)\rangle|^2 \approx |\langle j |\psi(\tau/4 - \Delta t)\rangle|^2 \quad (41)$$

i.e., the reflection process is symmetric about the instant $t = \tau/4$. We refer this phenomena as to elastic reflection due to the fact that it is analog to a mass-spring system in classical physics.

On the other hand, the dynamics before reflection is the same for an initial state located in anywhere of the chain. Then the elastic reflection also happens for the initial state with $\kappa_0 \neq \pi/2$. We will show that the combination of two such features leads to a probability preserving dynamics which usually appears in a Hermitian system. Such a process occurs when consider an initial state locates far from the center of the chain. As extension of the wave packet, one of its edges moves in opposite direction after the elastic bounce from one end of the chain. Then two edges of the wave packet move in the same direction with the same speed, which results in a translational motion of the wave packet, preserving the Dirac probability. Fig. 6 Plot of profile evolved state for initial state with $\kappa_0 \neq \pi/2$.

Now we consider the time evolution for initial state as a superposition of two wave packets. Such an investigation is trivial for a Hermitian system. However, some unexpected phenomena may be found in a non-Hermitian system although it is also a linear system. This is because

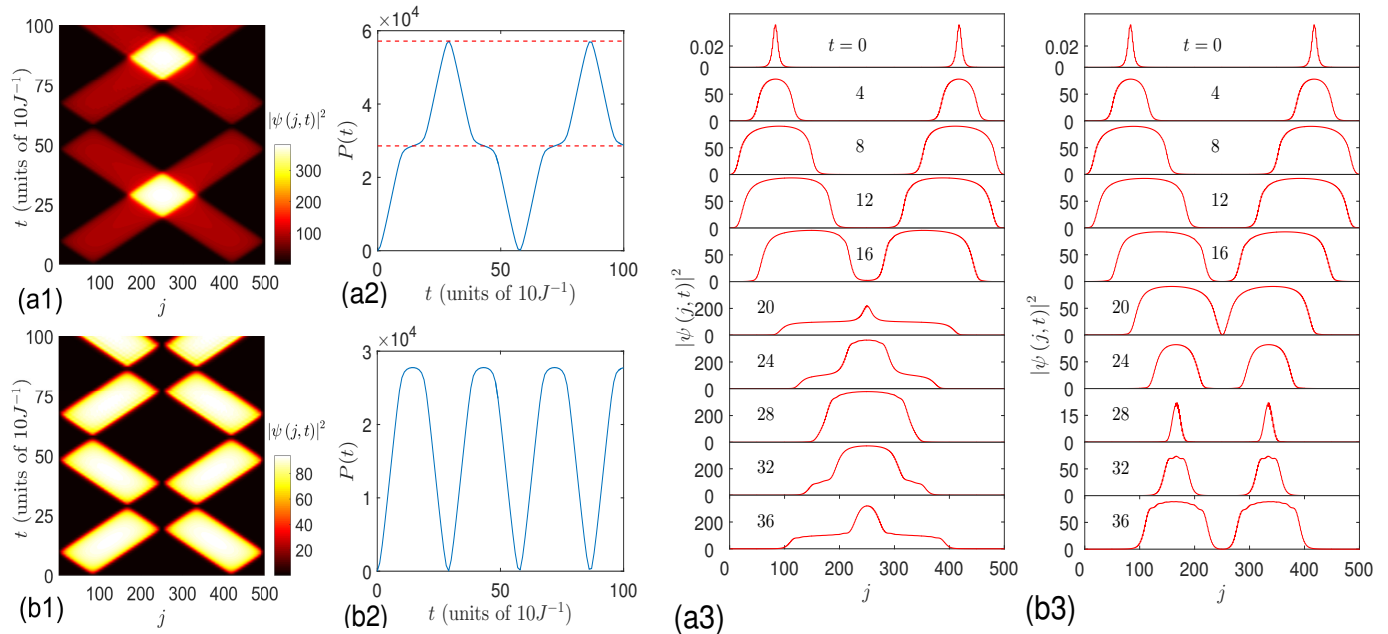


FIG. 7. (Color online) The same as that in Fig. 6, but for initial states (a1) $|\Psi_+\rangle$ and (b1) $|\Psi_-\rangle$ expressed in Eq. (42) with $\kappa_{01} = \pi/6$, $\kappa_{02} = 5\pi/6$, obtained by numerical simulation. (a2) and (b2) are plots of $P(t)$ for the time evolutions for (a1) and (b1), respectively. (a3) and (b3) are the profiles of the evolved wave packets at several typical instants for (a1) and (b1), respectively. We see that when two wave packets are separated, the total probability is always constant, while changes when they overlap. In the case of (a2), the probability doubles as indicated by two dotted lines. It is due to the anomalous interference phenomenon, in which there are no interference patterns. In contrast, from (b2) we see that the probability turns to very small, as if two wave packets annihilate together, or absorb each other. It is a peculiar dynamics, no counterpart in Hermitian system.

the Dirac probability is not defined by a canonical inner product (biorthonormal inner product). The initial state is taken in the form

$$|\Psi_{\pm}\rangle = \frac{\Lambda}{\sqrt{2}} \sum_{n=1, \sigma=\pm} \sigma [\sin(n\kappa_{01}) \pm \sin(n\kappa_{02})] \times \frac{\exp(-qn)}{n} |\psi_n^{\sigma}\rangle, \quad (42)$$

where κ_{01} and κ_{02} determine the initial locations of two wave packets. The trajectories and profiles of two wave packets are clear when they do not overlap. We are interested in what happens when they meet together. To answer this question, we employ the numerical simulation to compute the probability of the evolved state. Fig. 7, shows that the dynamics of $|\Psi_+\rangle$ behaves as a Hermitian one, while $|\Psi_-\rangle$ exhibits a peculiar behavior: It looks like that two wave packets cancel each other out when they meet together.

VI. SUMMARY

In summary, we have investigated the non-Hermitian analogue of an active laser medium, and find a scenario for the mechanism of lasing in the framework of quantum

mechanics. We have proposed alternative lasing mechanism induced by the EP in a finite non-Hermitian system rather than SS in an infinite system with a non-Hermitian scattering center. The key difference between two mechanisms is that a laser can be fired everywhere on the former while only at the scattering center in the latter. The present non-Hermitian system also exhibits many peculiar dynamic behaviors, such as elastic reflection, collision and probability preserving translational propagation, etc. The underlying mechanism of such features is the balance of distortion and staggered imaginary potentials, while an SS laser solution does not require the balance. In general, the position of EPs are a little different for a same model but with different boundary conditions, or more generally speaking, with and without some defects. When the initial state is local in coordinate space, its dynamics within certain period of time is independent of the boundary condition and its initial location. This provides a way to explore the dynamics, which is the combination of a quasi-Hermitian and Jordan block time evolutions in a general non-Hermitian system. So the key point in practice is the specific class of initial states. For the present model, the linear increase of probability arises from such a combination. It can be seen from the

nonzero overlap

$$|\langle \phi_c | \psi(0) \rangle| \approx \frac{\sqrt{\delta(1-\delta)}\Lambda}{N\delta} \arctan\left(\frac{\sin \kappa_0}{\sinh q}\right), \quad (43)$$

where

$$|\phi_c\rangle = \frac{1}{\sqrt{2N}} \sum_{j=1}^N (-1)^j (|2j-1\rangle + i|2j\rangle), \quad (44)$$

is the coalescing eigen vector of the conjugate Hamiltonian H^\dagger in Eq. (1) with periodic boundary condition.

Our results, on the one hand, provide an alternative losing theory in the context of non-Hermitian quantum mechanics, on the other hand, indicates non-Hermitian system is a fertile ground for many unknown features in physics.

ACKNOWLEDGMENTS

This work was supported by National Natural Science Foundation of China (under Grant No. 11874225).

-
- [1] C. M. Bender and S. Boettcher, Phys. Rev. Lett. **80**, 5243 (1998).
- [2] C. M. Bender, S. Boettcher, and P. N. Meisinger, J. Math. Phys. **40**, 2201 (1999).
- [3] P. Dorey, C. Dunning, and R. Tateo, J. Phys. A: Math. Gen. **34**, L391 (2001).
- [4] P. Dorey, C. Dunning, and R. Tateo, J. Phys. A: Math. Gen. **34**, 5679 (2001).
- [5] C. M. Bender, D. C. Brody, and H. F. Jones, Phys. Rev. Lett. **89**, 270401 (2002).
- [6] A. Mostafazadeh, J. Math. Phys. **43**, 3944 (2002).
- [7] A. Mostafazadeh, J. Phys. A: Math. Gen. **36**, 7081 (2003).
- [8] H. F. Jones, J. Phys. A: Math. Gen. **38**, 1741 (2005).
- [9] M. Znojil, J. Phys. A **40**, 13131 (2007).
- [10] M. Znojil, J. Phys. A **41**, 292002 (2008).
- [11] M. Znojil, Phys. Rev. A **82**, 052113 (2010).
- [12] A. Guo, Phys. Rev. Lett. **103**, 093902 (2009).
- [13] C. E. Rüter, et al. Nat. Phys. **6**, 192-195 (2010).
- [14] W. Wan, Y. Chong, L. Ge, H. Noh, A. D. Stone, and H. Cao, Science **331**, 889-892 (2011).
- [15] Y. Sun, W. Tan, H.-Q. Li, J. Li, and H. Chen, Phys. Rev. Lett. **112**, 143903 (2014).
- [16] L. Feng, et al. Nature Mater. **12**, 108-113 (2013).
- [17] B. Peng, et al. Nat. Phys. **10**, 394-398 (2014).
- [18] L. Chang, et al. Nature Photon. **8**, 524-529 (2014).
- [19] L. Feng, Z. J. Wong, R.-M. Ma, Y. Wang, and X. Zhang, Science **346**, 972-975 (2014).
- [20] H. Hodaei, et al. Science **346**, 975-978 (2014).
- [21] M. Wimmer, et al. Nat. Commun **6**, 7782 (2015).
- [22] J. G. Muga, J. P. Palaob, B. Navarro, and I. L. Egusquiza, Phys. Rep. **395**, 357 (2004).
- [23] A. Guo, G. J. Salamo, D. Duchesne, R. Morandotti, M. Volatier-Ravat, V. Aimez, G. A. Siviloglou, and D. N. Christodoulides, Phys. Rev. Lett. **103**, 093902 (2009).
- [24] K. G. Makris, R. El-Ganainy, D. N. Christodoulides, and Z. H. Musslimani, Phys. Rev. Lett. **100**, 103904 (2008).
- [25] Z. H. Musslimani, K. G. Makris, R. El-Ganainy, D. N. Christodoulides, Phys. Rev. Lett. **100**, 030402 (2008).
- [26] B. Peng, S. K. Özdemir, F. Lei, F. Monifi, M. Gianfreda, G. L. Long, S. Fan, F. Nori, C. M. Bender, and L. Yang, Nat. Phys. **10**, 394 (2014).
- [27] L. Feng, Z. J. Wong, R.-M. Ma, Y. Wang, and X. Zhang, Science **346**, 972 (2014).
- [28] H. Hodaei, M.-A. Miri, M. Heinrich, D. N. Christodoulides, and M. Khajavikhan, Science **346**, 975 (2014).
- [29] Z. Lin, A. Pick, M. Loncar, and A. W. Rodriguez, Phys. Rev. Lett. **117**, 107402 (2016).
- [30] J. Wiersig, Phys. Rev. A **93**, 033809 (2016).
- [31] Y. L. Liu, R. B. Wu, J. Zhang, S. K. Özdemir, L. Yang, F. Nori, and Y. X. Liu, Phys. Rev. A **95**, 013843 (2017).
- [32] X. Z. Zhang, L. Tian, and Y. Li, Phys. Rev. A **97**, 043818 (2018).
- [33] W. H. Hu, L. Jin, Y. Li, and Z. Song, Phys. Rev. A **86**, 042110, (2012).
- [34] K. L. Zhang, P. Wang, G. Zhang, and Z. Song, Phys. Rev. A **98**, 022128, (2018).
- [35] J. K. Asbóth, L. Oroszlány, A. Pályi, Lecture Notes in Physics, **919** (2016).
- [36] Simon Malzard, Charles Poli, and Henning Schomerus, Phys. Rev. Lett. **115**, 200402 (2015).
- [37] Huaiming Guo and Shu Chen, Phys. Rev. B **91**, 041402(R) (2015).
- [38] Linhu Li and Shu Chen, Phys. Rev. B **92**, 085118 (2015).
- [39] Peng Peng, Wanxia Cao, Ce Shen, Weizhi Qu, Jianming Wen, Liang Jiang, and Yanhong Xiao, Nat. Phys. **12**, 1139 (2016).
- [40] Tony E. Lee, Phys. Rev. Lett. **116**, 133903 (2016).
- [41] S. Lin, and Z. Song, Phys. Rev. A **96**, 052121 (2017).
- [42] E. M. Graefe, H. J. Korsch, and A. E. Niederle, Phys. Rev. A **82**, 013629 (2010).
- [43] E. M. Graefe, H. J. Korsch, and A. E. Niederle, Phys. Rev. Lett. **101**, 150408 (2008).
- [44] H. Cartarius and N. Moiseyev, Phys. Rev. A **84**, 013419 (2011).
- [45] X. Z. Zhang, L. Jin, and Z. Song, Phys. Rev. A **85**, 012106 (2012).